

# Quasiparticle Energy Dispersion and Shadow Peaks in a Doped $SO(5)$ Symmetric Ladder

Seung-Pyo Hong and Sung-Ho Suck Salk

*Department of Physics, Pohang University of Science and Technology, Pohang 790-784, Korea*

## Abstract

Mean field and exact diagonalization studies on the quasiparticle excitation of an  $SO(5)$  symmetric two-leg ladder system are reported. It is shown that the energy gap in the quasiparticle excitation is caused by the formation of rung singlet states. We find that shadow peaks can occur above the Fermi surface with antiferromagnetic electron correlations involving only rungs in the spin ladder.

PACS numbers: 74.25.Jb, 74.25.-q, 71.10.-w, 71.27.+a

The cuprate materials of high critical superconducting temperatures exhibit antiferromagnetism near half-filling and superconductivity away from half filling. Zhang [1,2] suggested that the two phenomena are manifestations of the same thing and can be explained in a unified framework based on  $SO(5)$  symmetry. Recently Scalapino et al. [3] presented a simple  $SO(5)$  model on a two-leg ladder system which can be served as a toy model to investigate various physics involving the  $SO(5)$  symmetry. In this paper we discuss quasiparticle excitations for the  $SO(5)$  two-leg spin ladder from both analytic and numerical results. We derive a mean field quasiparticle energy dispersion relation. For a through comparison one-particle spectral function is calculated by applying a Lanczos exact diagonalization method to a ladder of  $2 \times 6$  sites. We find that the energy gap in the quasiparticle excitations is largely contributed by the formation of rung singlet states. We also find the appearance of shadow peaks with Heisenberg interaction along rungs alone.

The  $SO(5)$  symmetric two-leg ladder Hamiltonian is given by [3]

$$\begin{aligned}
H = & -t_{\parallel} \sum_{i\lambda\sigma} (c_{i\lambda\sigma}^\dagger c_{i+1\lambda\sigma} + \text{H.c.}) - t_{\perp} \sum_{i\sigma} (c_{i1\sigma}^\dagger c_{i2\sigma} + \text{H.c.}) \\
& + U \sum_{i\lambda} \left( n_{i\lambda\uparrow} - \frac{1}{2} \right) \left( n_{i\lambda\downarrow} - \frac{1}{2} \right) + V \sum_i (n_{i1} - 1)(n_{i2} - 1) \\
& + J \sum_i \mathbf{S}_{i1} \cdot \mathbf{S}_{i2} - \mu \sum_{i\lambda\sigma} n_{i\lambda\sigma}
\end{aligned} \tag{1}$$

Here  $c_{i\lambda\sigma}^\dagger$  creates an electron with spin  $\sigma$  on the  $i$ -th rung of the  $\lambda$ -th leg with  $i = 1, \dots, L$  and  $\lambda = 1, 2$ .  $n$  is the number operator,  $n_{i\lambda\sigma} = c_{i\lambda\sigma}^\dagger c_{i\lambda\sigma}$ ,  $n_{i\lambda} = \sum_{\sigma} n_{i\lambda\sigma}$ , and  $\mathbf{S}$  is the spin operator,  $\mathbf{S}_{i\lambda} = \frac{1}{2} c_{i\lambda\alpha}^\dagger \boldsymbol{\sigma}_{\alpha\beta} c_{i\lambda\beta}$ .  $t_{\parallel}$  is the hopping integral in the leg direction;  $t_{\perp}$ , the hopping integral in the rung direction;  $U$ , the on-site Coulomb interaction;  $V$ , the near-neighbor Coulomb interaction on a rung;  $J$ , the Heisenberg exchange interaction on a rung; and  $\mu$ , the chemical potential. The Heisenberg interaction of the  $SO(5)$  ladder Hamiltonian allows both singly and doubly occupied sites, while that of the  $t$ - $J$  ladder Hamiltonian allows only singly occupied sites. The constraint for the interaction strengths,  $J = 4(U + V)$  in Eq. (1) above is required for the  $SO(5)$  symmetry.  $U$  and  $V$  can be repulsive or attractive potentials. In the present study we will consider only the case of repulsive potentials,  $U \geq 0$  and  $V \geq 0$ ,

which is in the region of the  $E_0$  spin gap phase (represented by the tensor product of rung singlet states in the strong coupling limit) defined by Scalapino et al. [3]

The weak coupling (that is,  $U, V \ll t_{\parallel} \simeq t_{\perp}$ ) may allow linearization of the Coulomb repulsion terms

$$\begin{aligned} & \left( n_{i\lambda\uparrow} - \frac{1}{2} \right) \left( n_{i\lambda\downarrow} - \frac{1}{2} \right) \\ &= \left\langle n_{i\lambda\uparrow} - \frac{1}{2} \right\rangle \left( n_{i\lambda\downarrow} - \frac{1}{2} \right) + \left\langle n_{i\lambda\downarrow} - \frac{1}{2} \right\rangle \left( n_{i\lambda\uparrow} - \frac{1}{2} \right) - \left\langle n_{i\lambda\uparrow} - \frac{1}{2} \right\rangle \left\langle n_{i\lambda\downarrow} - \frac{1}{2} \right\rangle \end{aligned}$$

and

$$\begin{aligned} & (n_{i1} - 1)(n_{i2} - 1) \\ &= \langle n_{i1} - 1 \rangle (n_{i2} - 1) + \langle n_{i2} - 1 \rangle (n_{i1} - 1) - \langle n_{i1} - 1 \rangle \langle n_{i2} - 1 \rangle \end{aligned}$$

Taking into account  $\langle n_{i\lambda\uparrow} \rangle = \langle n_{i\lambda\downarrow} \rangle = \frac{1-\delta}{2}$  with  $\delta$ , the doping rate, which neglects hole density fluctuations, we write the Coulomb repulsions  $(n_{i\lambda\uparrow} - \frac{1}{2})(n_{i\lambda\downarrow} - \frac{1}{2}) = -\frac{\delta}{2}n_{i\lambda} + \frac{\delta}{2} - \frac{\delta^2}{4}$  and  $(n_{i1} - 1)(n_{i2} - 1) = -\delta(n_{i1} + n_{i2}) + 2\delta - \delta^2$ , and add them to the chemical potential term in Eq. (1). The Heisenberg interaction can be written [4] as

$$\begin{aligned} \mathbf{S}_{i1} \cdot \mathbf{S}_{i2} &= -\frac{3}{8}[\chi_{i12}^*(c_{i1\uparrow}^*c_{i2\uparrow} + c_{i1\downarrow}^*c_{i2\downarrow}) + \text{H.c.}] + \frac{3}{8}n_{i1} \\ &\quad -\frac{3}{8}[\Delta_{i12}^*(c_{i1\uparrow}c_{i2\downarrow} - c_{i1\downarrow}c_{i2\uparrow}) + \text{H.c.}] \end{aligned}$$

where the hopping order parameter is  $\chi_{i12} = \langle c_{i1\uparrow}^*c_{i2\uparrow} + c_{i1\downarrow}^*c_{i2\downarrow} \rangle$  and the singlet pair order parameter,  $\Delta_{i12} = \langle c_{i1\uparrow}c_{i2\downarrow} - c_{i1\downarrow}c_{i2\uparrow} \rangle$ . We take  $\chi_{i12} = \chi$  and  $\Delta_{i12} = \Delta$  by neglecting spatial fluctuations of both the amplitude and the phase. The mean field Hamiltonian is then in momentum space,

$$\begin{aligned} H &= \sum_{k\lambda\sigma} (-2t_{\parallel} \cos k_x - \mu) c_{k\lambda\sigma}^* c_{k\lambda\sigma} - t_{\perp} \sum_{k\sigma} (c_{k1\sigma}^* c_{k2\sigma} + \text{H.c.}) \\ &\quad - \frac{3J}{8} \sum_k [\chi^*(c_{k1\uparrow}^* c_{k2\uparrow} + c_{k1\downarrow}^* c_{k2\downarrow}) + \Delta^*(c_{k1\uparrow} c_{k2\downarrow} - c_{k1\downarrow} c_{k2\uparrow}) + \text{H.c.}] \end{aligned} \quad (2)$$

The quasiparticle energy dispersion is readily obtained from Eq. (2) above,

$$E_k = \pm \sqrt{\left[ (-2t_{\parallel} \cos k_x - \mu) \pm \left( t_{\perp} + \frac{3J\chi}{8} \right) \right]^2 + \left( \frac{3J\Delta}{8} \right)^2} \quad (3)$$

The mean field order parameters  $\chi$ ,  $\Delta$ , and the chemical potential  $\mu$  are obtained from self-consistent equations. For the time being we take the values of  $\chi$ ,  $\Delta$ , and  $\mu$  obtained from our Lanczos calculations on the  $2 \times 6$  ladder with two doped holes. The quasiparticle energy dispersion is shown in Fig. 1; the bonding band (denoted as B) has its minimum energy at  $k_x = 0$  with the Fermi surface at  $k_F^B \simeq \frac{2\pi}{3}$ , while the antibonding band (denoted as A) has its minimum energy at  $k_x = 0$  with the Fermi surface at  $k_F^A \simeq \frac{\pi}{3}$ . Splitting between the two bands, that is, the removal of degeneracy is caused by hopping (overlap) integral  $t_{\perp}$  in the rung direction. The bonding band is pushed down with more occupied electrons, while the antibonding band is pushed up with less occupied electrons. We note that with  $k_F^B > k_F^A$  the Luttinger sum rule is satisfied, that is,  $k_F^B + k_F^A = (1 - \delta)\pi$ . The dashed parts of the dispersion curves in Fig. 1 represent the shadow bands in our two-leg ladder system which is similar to the ones discussed in two-dimensional planar systems [5–7]. As shown in Eq. (3) the shadow band in Fig. 1 is largely contributed by the Heisenberg interaction in the rung direction, while the shadow band in the two-dimensional planar systems [5–7] is caused by antiferromagnetic correlations whose strengths are equal in both the horizontal and vertical directions.

To examine the single particle excitations, we write in the case of two-hole doped system of  $2 \times L$  sites [8],

$$A_e(\mathbf{k}, \omega) = \sum_{\alpha} \left| \langle \Psi_{\alpha}^{2L-1} | c_{\mathbf{k}\sigma}^{\dagger} | \Psi_0^{2L-2} \rangle \right|^2 \delta(\omega - E_{\alpha}^{2L-1} + E_0^{2L-2} + \mu) \quad (4.a)$$

for the particle spectral function ( $\omega > 0$ ) and

$$A_h(\mathbf{k}, \omega) = \sum_{\alpha} \left| \langle \Psi_{\alpha}^{2L-3} | c_{\mathbf{k}\sigma} | \Psi_0^{2L-2} \rangle \right|^2 \delta(-\omega - E_{\alpha}^{2L-3} + E_0^{2L-2} - \mu) \quad (4.b)$$

for the hole spectral function ( $\omega < 0$ ). Here  $|\Psi_{\alpha}^N\rangle$  is the  $\alpha$ -th eigenstate in the subspace of  $N$  electrons with the eigenenergy  $E_{\alpha}^N$ . The chemical potential is defined as  $\mu = \frac{1}{2}(E_0^{2L-1} - E_0^{2L-3})$ . We calculate the spectral function by using both the Lanczos method and the continued fraction approach [9]. The results are shown in Fig. 2 for  $L = 6$ ,  $t_{\parallel} = t_{\perp} = 1$  and  $V = 0$ , as a function of  $U$  and  $J$ . The coupling strengths,  $U$  and  $J$  are related to each other and  $J$  increases faster than  $U$  due to the  $SO(5)$  constraint,  $J = 4(U + V) = 4U$ .

We now investigate the spectral functions by varying the values of  $U$  (and consequently  $J$ ). First the computed free particle spectral functions for the case of  $U = J = 0$  are shown in Fig. 2(a). The Fermi momentum of the bonding ( $k_y = 0$ ) band is  $k_F^B = \frac{2\pi}{3}$ , and that of the antibonding ( $k_y = \pi$ ) band is  $k_F^A = \frac{\pi}{3}$ . Below the Fermi surface, we observe sharp and well-defined quasiparticle peaks for both the bonding and the antibonding bands. All the single particle states below the Fermi surface are occupied, and there exist no spectral peaks above the Fermi surface. The computed spectral functions shown in Fig. 2(a) are seen to agree well with the free particle energy dispersion,  $\varepsilon_k = -2t_{\parallel} \cos k_x \pm t_{\perp}$  in Eq. (3).

The spectral functions for the case of small coupling strengths,  $U = 0.1$  and  $J = 0.4$  are displayed in Fig. 2(b). The predicted Fermi momenta are found at  $k_F^B \simeq \frac{2\pi}{3}$  and  $k_F^A \simeq \frac{\pi}{3}$  in agreement with the mean field result given by Eq. (3). The calculated positions of the quasiparticle peaks below the Fermi surface are also in good agreement with the analytic mean field result of Eq. (3). Although the interaction strengths are small, interestingly enough there appear spectral peaks above the Fermi momentum (surface). Such peaks are the shadow peaks which were also observed by others [10]. The peak in the bonding band with momentum  $(\pi, 0)$  above the Fermi surface is a shadow of the peak belonging to the antibonding band with momentum  $(0, \pi)$  which is below the Fermi surface. The peak with momentum  $(\frac{2\pi}{3}, \pi)$  is a shadow of the peak with momentum  $(-\frac{\pi}{3}, 0)$  (degenerate at  $(\frac{\pi}{3}, 0)$ ), and the peak with momentum  $(\pi, \pi)$  is a shadow of the peak with momentum  $(0, 0)$ . Haas and Dagotto [10] reported the presence of shadow peaks in  $t$ - $J$  ladder systems and concluded that short-range antiferromagnetic correlations are responsible for the shadow peaks in the spin ladder system.

In order to investigate which of the two parameters  $U$  and  $J$  is more responsible for yielding the shadow peaks, we first set  $J = 0$  and calculate spectral functions for several cases of  $U$  as shown in Fig. 3. We note that the stronger the on-site Coulomb repulsion, the broader the bonding orbital becomes, which is more evident for the orbitals, particularly at lower values of  $k_x$  (substantially below the Fermi surface), for example, at  $k = (0, 0)$  and

$(\frac{\pi}{3}, 0)$  as shown in Fig. 3. The overall structure of the bonding and the antibonding bands does not change much with increasing  $U$ . We find that the shadow peaks can be generated even with a small Coulomb repulsion  $U = 0.1$  as shown in Fig. 3(b). While Haas and Dagotto's results [10] are based on the strong coupling limit  $U \gg t$  due to the use of the  $t$ - $J$  Hamiltonian, we discover the shadow peaks in both the weak and the strong coupling limits. Second order hopping processes generates an effective interaction of strength  $\sim t^2/U$  between the electrons on nearest-neighbor sites. Since the hopping integral along the rung ( $t_{\perp}$ ) and that along the chain ( $t_{\parallel}$ ) are the same, it is hard to determine from their study which direction of electron correlations is more important for the shadow peaks.

In order to thoroughly verify the validity of shadow peaks caused essentially by the antiferromagnetic correlation between the two electrons in the rung, namely, by the spin singlet state along the rung direction, we computed the spectral functions for the case of  $U = V = 0$ ,  $J_{\perp} \equiv J \neq 0$  and  $J_{\parallel} = 0$  as shown in Fig. 4. We find that the shadow peaks appear above the Fermi surface with the Heisenberg interaction along rungs alone as displayed in Fig. 4(b). Thus the singlet bonding on the rungs is responsible for the presence of the shadow peaks.

Now we reexamine the  $SO(5)$  symmetric cases of  $J = 4U$ . The spectral functions for different values of  $U$  and  $J$  are shown in Figs. 2(c),(d),(e). As  $J$  increases, the energies of the bonding and the antibonding orbitals decrease with increasing energy gap. It is to be reminded that due to the  $SO(5)$  constraint to define the relation between  $J$  and  $U$ ,  $J$  increases more rapidly (4 times faster) than  $U$ . Thus it is of great interest to see how the spectral positions and energy gaps vary as a result of larger contribution by  $J$ . As can be seen from the comparison of Figs. 2 and 3, we note that the energy gap is largely contributed by  $J$ , but not substantially so by  $U$ . The dominance of spin singlet states on the rungs for the determination of the energy gap is manifest from this study. Indeed this observation is in good accordance with the mean field prediction; the energy gap is caused by the Heisenberg interaction  $J$  as shown in Eq. (3).

The dispersion of the bonding band does not greatly change with increasing values of  $J$ ,

in contrast to that of the antibonding band. As  $J$  increases, the antibonding band is lowered more rapidly than the bonding band and finally becomes dispersionless (no dependence on  $k_x$ ) as shown in Fig. 2(e). The Heisenberg interaction  $J$ , which is taken to be anisotropic due to  $J_{\perp} \neq 0$  and  $J_{\parallel} = 0$ , obviously favors the formation of the local rung singlet. The rung singlets are clearly local because there exists no phase coherence between the singlets on the adjacent rungs, which, in turn, causes the appearance of the dispersionless antibonding band.

We have investigated quasiparticle excitations in the  $SO(5)$  symmetric two-leg ladder system recently proposed by Scalapino et al. [3] The quasiparticle energy dispersion is discussed in both the mean field approach and the exact diagonalization study. The dispersion consists of two branches, the bonding band with Fermi momentum  $k_F^B \simeq \frac{2\pi}{3}$  and the anti-bonding band with Fermi momentum  $k_F^A \simeq \frac{\pi}{3}$ . The hole spectral functions calculated from the Lanczos exact diagonalization method were found to agree well with the mean field results. The formation of rung singlet states is responsible for the energy gap in the quasiparticle excitations. Finally we find that the presence of shadow peaks above the Fermi surface can essentially occur as a result of the singlet bonding on the rungs, indicating that the on-site Coulomb repulsion along chains or rungs may not be a prime cause for the formation of shadow peaks.

One of us (S.H.S.S) acknowledges the financial supports of Korean Ministry of Education (BSRI-97) and of the Center for Molecular Sciences at KAIST.

## REFERENCES

- [1] S.-C. Zhang, *Science* **275**, 1089 (1997); S.-C. Zhang, *Physica C* **282-287**, 265 (1997)
- [2] S. Meixner, W. Hanke, E. Demler, and S.-C. Zhang, *Phys. Rev. Lett.* **79**, 4902 (1997); S. Rabello, H. Kohno, E. Demler, and S.-C. Zhang, *Phys. Rev. Lett.* **80**, 3586 (1998); R. Eder, W. Hanke, and S.-C. Zhang, *Phys. Rev. B* **57**, 13781 (1998)
- [3] D. J. Scalapino, S.-C. Zhang, and W. Hanke, *Phys. Rev. B* **58**, 443 (1998)
- [4] M. U. Ubbens and P. A. Lee, *Phys. Rev. B* **46**, 8434 (1992)
- [5] A. P. Kampf and J. R. Schrieffer, *Phys. Rev. B* **42**, 7967 (1990); *Phys. Rev. B* **41**, 6399 (1990)
- [6] P. Aebi, J. Osterwalder, P. Schwaller, L. Schlapbach, M. Shimoda, T. Mochiku, and K. Kadowaki, *Phys. Rev. Lett.* **72**, 2757 (1994)
- [7] S. Haas, A. Moreo, and E. Dagotto, *Phys. Rev. Lett.* **74**, 4281 (1995)
- [8] H. Tsunetsugu, M. Troyer, and T. M. Rice, *Phys. Rev. B* **49**, 16078 (1994); M. Troyer, H. Tsunetsugu, and T. M. Rice, *Phys. Rev. B* **53**, 251 (1996)
- [9] E. Dagotto, *Rev. Mod. Phys.* **66**, 763 (1994)
- [10] S. Haas and E. Dagotto, *Phys. Rev. B* **54**, 3718 (1996)

## FIGURE CAPTIONS

FIG. 1. The quasiparticle energy dispersion obtained by using the mean field approach in the weak coupling limit. The parameters are chosen from our Lanczos calculations on a  $2 \times 6$  ladder with two doped holes as  $t_{\parallel} = t_{\perp} = 1$ ,  $J = 0.4$ ,  $\chi = 0.47$ ,  $\Delta = -0.15$ ,  $\mu = -0.099$ . B denotes a bonding ( $k_y = 0$ ) band and A, an antibonding ( $k_y = \pi$ ) band. The dashed parts of the dispersions denote shadow bands.

FIG. 2. Exact diagonalization results of the hole spectral function on a  $2 \times 6$  ladder with two doped holes for  $t_{\parallel} = t_{\perp} = 1$ ,  $V = 0$ , and several values of  $U$  and  $J$ . The dashed horizontal line denotes the Fermi energy, and the dotted arrows indicate the shadow peaks. The  $\delta$  functions have been given a finite width of  $\epsilon = 0.1$ .

FIG. 3. Same as in Fig. 2 but for  $J = 0$ .

FIG. 4. Same as in Fig. 2 but for  $U = 0$ .

## FIGURES

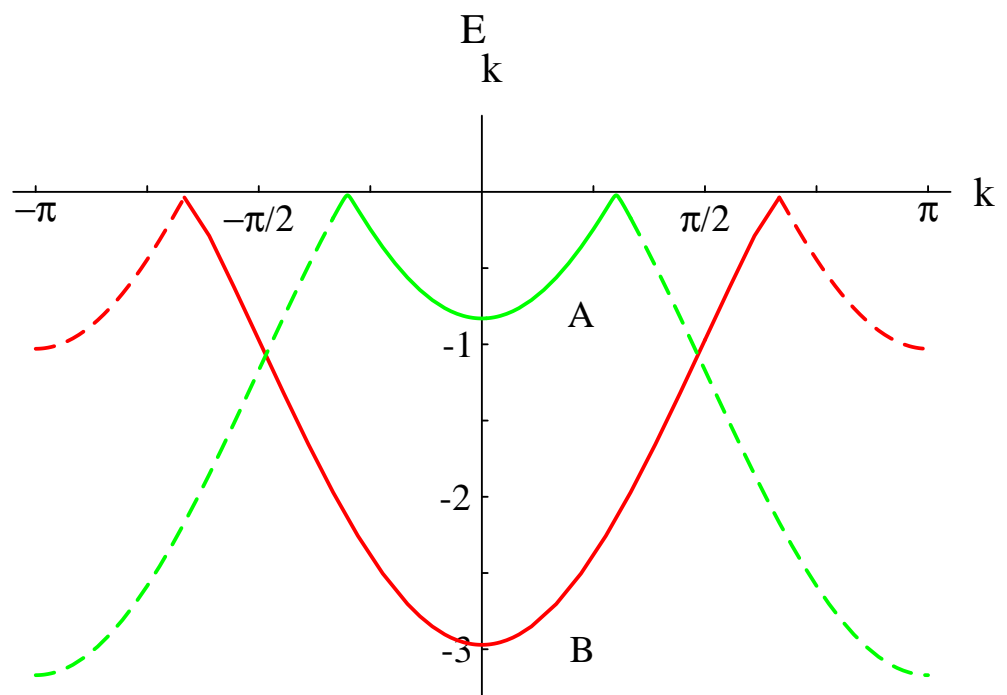


FIG. 1.

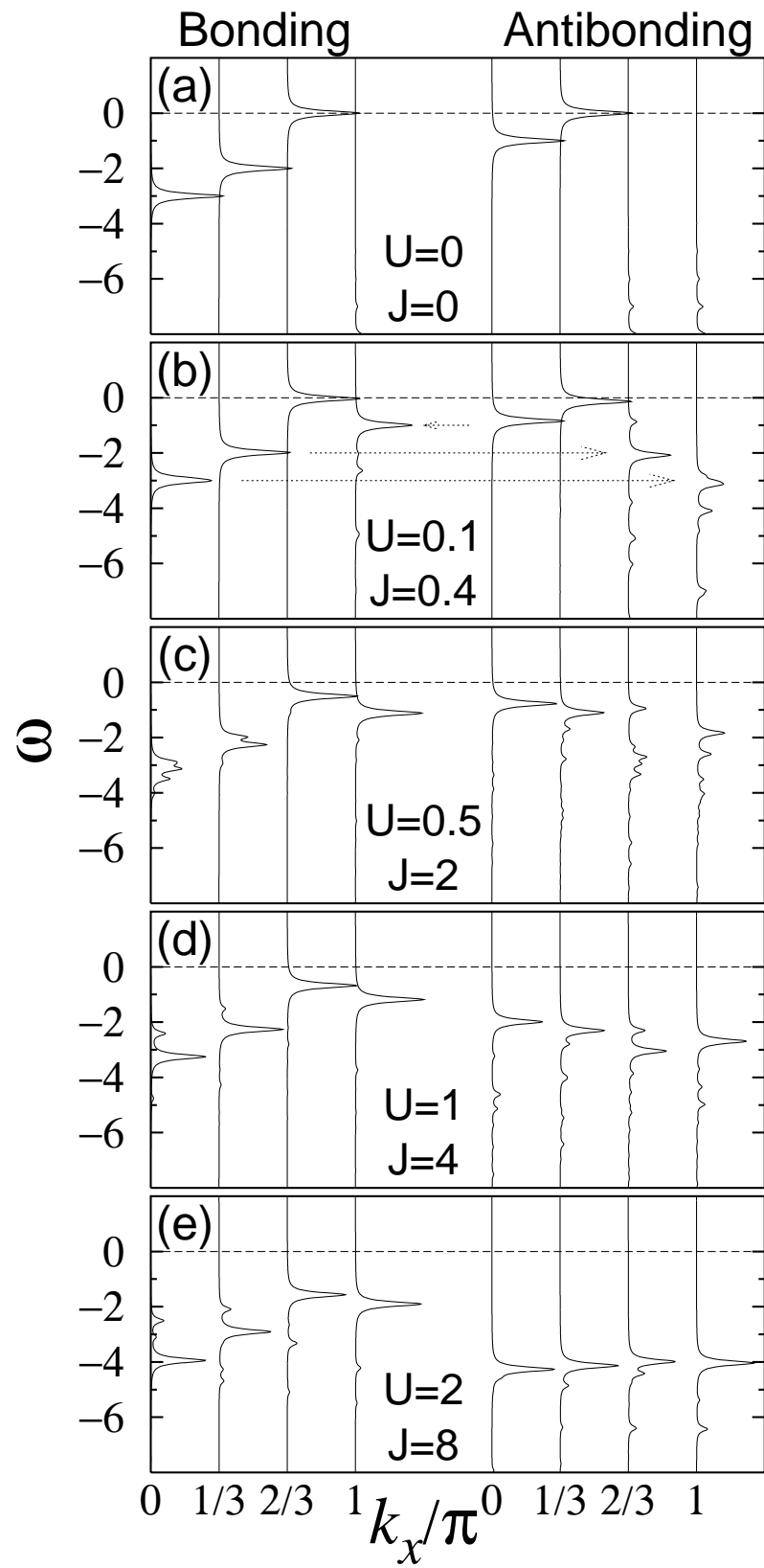


FIG. 2.

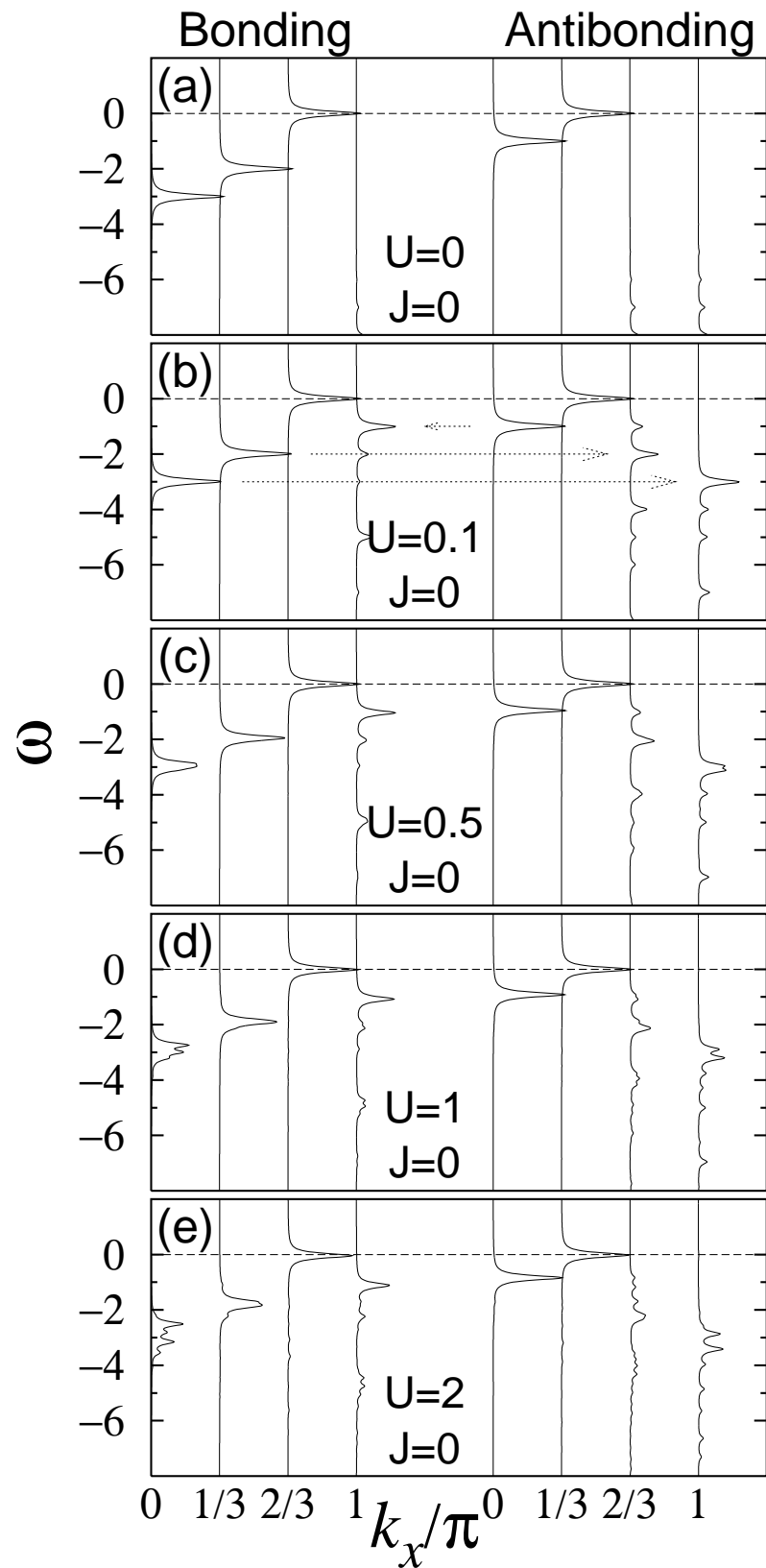


FIG. 3.

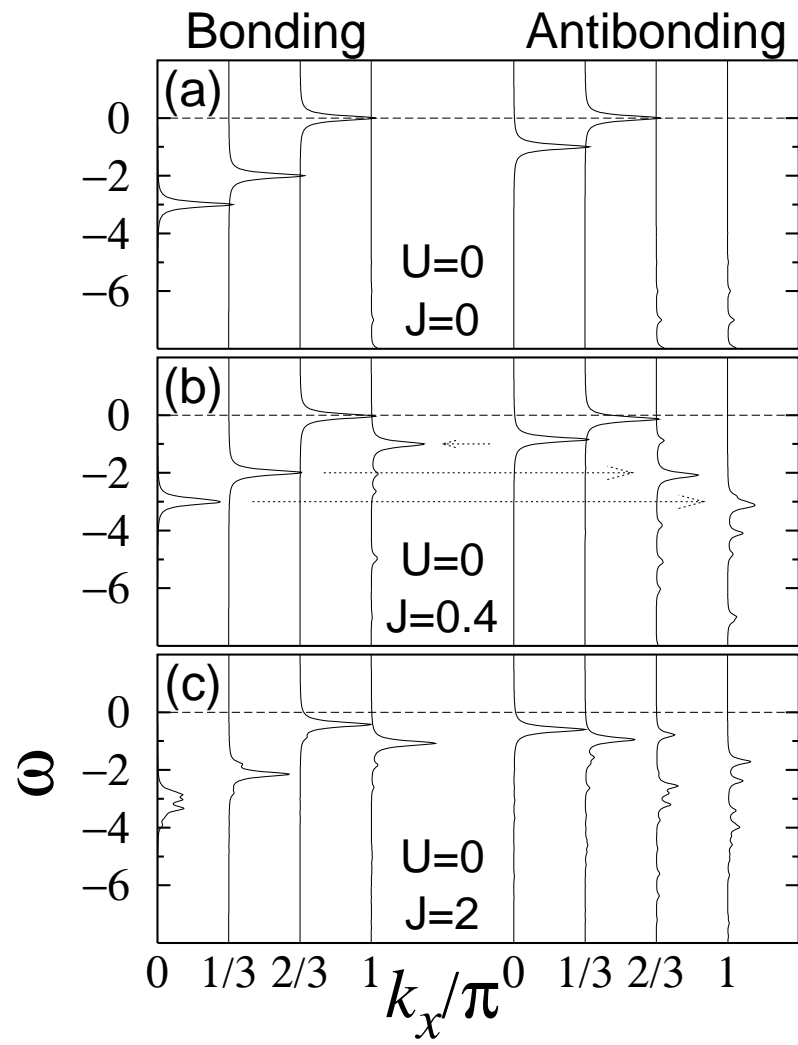


FIG. 4.